

# Professor A.I. Smirnov: a Visiting Fellowship: GR/S97927/01

## 1. Background Information

We received funding to support the visit of Prof. Alexander Smirnov to the Physics Department here at the University of Warwick. Prof. Smirnov worked in the Department for 6 months (May to August 2004 and March to April 2005). He was based in the laboratories of the Superconductivity and Magnetism Group and while his visit was most closely related to the research programme of Dr. Oleg Petrenko, he also worked with other research staff in this group.

Professor Smirnov is a leading scientist at P.L. Kapitza Institute for Physical Problems of the Russian Academy of Science. As originally planned, the three major aspects of Prof. Smirnov's visit into the Department were:

- use of research equipment available in the Department to extend our joint studies of frustrated and low dimensional magnetic systems. The research programme was centred around magnetisation and heat capacity measurements that were made using our Vibrating Sample Magnetometer (VSM) and SQUID magnetometer as well as a Physical Properties Measurement System (PPMS).
- Prof. Smirnov was a source for priceless advice during the final stages of setting up our new wide frequency range ESR (Electron Spin Resonance) laboratory here at Warwick. This project is funded by a separate EPSRC Grant GR/S08343. His experience and insight into how best to set up the ESR spectrometer has proved to be invaluable during the early phase operation of this apparatus.
- Prof. Smirnov was also able to consolidate further the research connections between the Kapitza Institute and the University of Warwick by writing joint publications and by preparing future research proposals.

## 2. Research Programme

The project was devoted to the investigation of new collective quantum states of magnetic systems. Two types of quantum spin liquids are at the focus of this study: low-dimensional magnetic materials (spin chains), and two- or three-dimensional magnets with geometrical frustration. The main topics of the project were: an investigation of the impurity-induced magnetic ordering in the Haldane magnet  $\text{PbNi}_2\text{V}_2\text{O}_8$ ; an investigation of the magnetic properties of a frustrated spin system on an ideal or distorted triangular lattice, in particular,  $\text{RbFe}(\text{MoO}_4)_2$ , and  $\text{KFe}(\text{MoO}_4)_2$  near the field induced incommensurate-commensurate phase transition.

In addition to these planned researched objectives, a significant portion of Prof. Smirnov's time at the University of Warwick was spent discussing the results and preparing the publications on our recent experiments on the adiabatic demagnetisation of a pyrochlore antiferromagnet  $\text{Gd}_2\text{Ti}_2\text{O}_7$ .

### 2.1. Field-controlled impurity induced ordering in the Haldane magnet $\text{Pb}(\text{Ni}_{1-x}\text{Co}_x)_2\text{V}_2\text{O}_8$ .

#### Introduction

Haldane spin chains (chains of magnetic  $S=1$  ions coupled by an antiferromagnetic exchange interaction) possess a quantum-disordered ground state with a finite correlation length. An important feature of this state is the energy gap separating the magnetic excited states from the disordered singlet ground state. This gap is of an exchange origin and can therefore stabilise a quantum disordered spin-liquid state in the presence of different perturbations causing magnetic ordering, such as an interchain exchange or anisotropy present in any real crystal. Several Haldane type spin-chain compounds are known at present. They demonstrate quantum spin-liquid states down to temperatures much lower than the temperature corresponding to the exchange energy – temperatures where regular 3D magnets or quasi 1D magnets with half-integer spins become magnetically ordered.

However, doping (including non-magnetic dilution) of the spin-gap quantum disordered systems is known to cause magnetic ordering. This specific effect is explained by the formation of local antiferromagnetically ordered areas appearing near the impurity atoms due to the antiferromagnetic

correlations. Furthermore, the local order parameters of these areas become coherent under the influence of a weak interchain interaction and due to their overlap. A fundamental feature of this nontrivial magnetic ordering is a strong dependence on the applied magnetic field. This dependence was found recently in our investigation of the impurity-induced ordering in the spin-Peierls magnet  $\text{CuGeO}_3$  [1]. The purpose of the investigations within the framework of this project was to look for possible effects of the application of a field on the impurity-induced transitions in the Haldane magnets.

## Results

The temperature of the impurity-induced magnetic ordering in ceramic samples of Co-doped  $\text{PbNi}_2\text{V}_2\text{O}_8$  was detected by measuring the temperature dependence of the specific heat. The measurements were performed using a Quantum Design PPMS calorimeter in magnetic fields up to 9 T. The temperature dependence of the specific heat is shown in Figs. 1 and 2 for two concentrations of impurities in  $\text{PbNi}_2\text{V}_2\text{O}_8$ . It was found that the Néel temperature is magnetic field dependent and also that a reduction of the Néel temperature under the action of the magnetic field is more pronounced for a smaller impurity concentration.

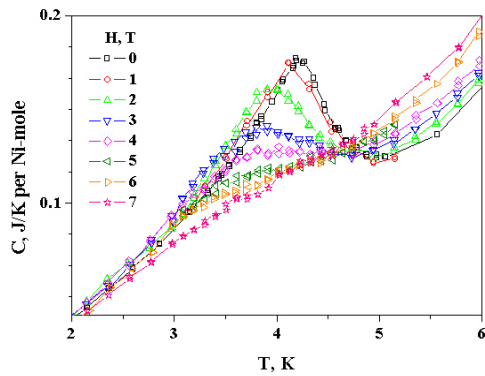


Fig. 1. Temperature dependence of the specific heat of the ceramic sample of  $\text{Pb}(\text{Ni}_{0.98}\text{Co}_{0.02})_2\text{V}_2\text{O}_8$

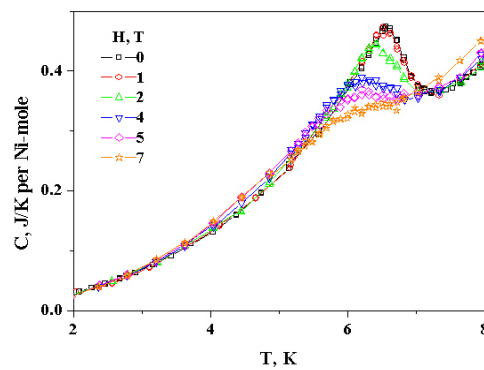


Fig. 2. Temperature dependence of the specific heat of the ceramic sample of  $\text{Pb}(\text{Ni}_{0.96}\text{Co}_{0.04})_2\text{V}_2\text{O}_8$

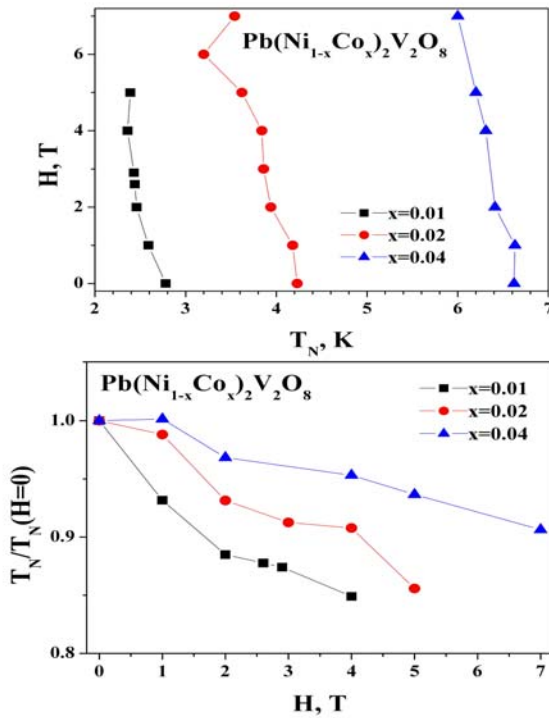


Fig. 3. Field dependences of the Néel temperature on the magnetic field.

This observation confirms the model developed in our  $\text{CuGeO}_3$  paper [1]. According to this model, a decoupling of the coherent antiferromagnetic areas is caused by the magnetic field due to a collective reorientation of spins neighbouring the impurity. This is because of the rotation of the total magnetic moment of the correlated areas to a position parallel to the external magnetic field. Figure 3 demonstrates the observed dependence of the Néel temperature on the magnetic field for several impurity concentrations. These dependences are more pronounced than previously reported by Masuda *et al.* [4] for Mg-doped samples. In particular, the concentration dependence of the  $dT_N/dH$  is clearly seen in our experiments with Co-doping and was not reported before.

## Resume

The measurements of the heat capacity of doped samples of a Haldane magnet revealed a strong influence of the external magnetic field on the impurity induced ordering, which is consistent with the model developed in ref. [1].

## 2.2. Investigation of the magnetic phase transitions in the triangular lattice antiferromagnet $\text{RbFe}(\text{MoO}_4)_2$

### Introduction

The problem of the magnetic ordering of two-dimensional triangular lattice antiferromagnets is of fundamental importance both for the studies of geometrically frustrated systems and also from the point of view of low-dimensional systems. The high degree of degeneracy of this spin system (preserved even in an applied magnetic field) results in the appearance of the specific field-induced phases, such as magnetisation plateau, stabilised by fluctuations [2]. The quasi two-dimensional antiferromagnet on a triangular lattice,  $\text{RbFe}(\text{MoO}_4)_2$  is a rare example of a crystal suitable for testing the theoretical models in this research area.

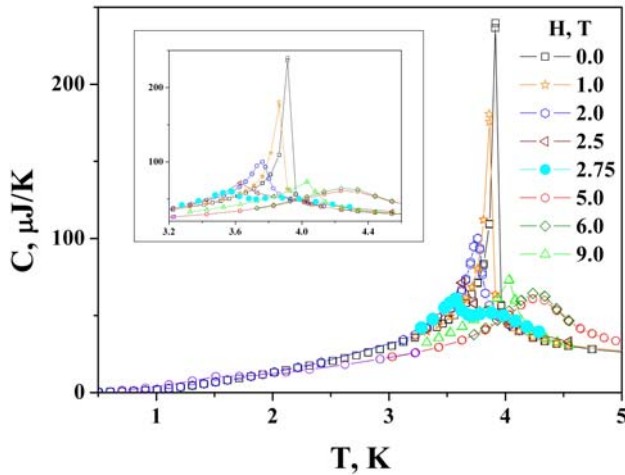
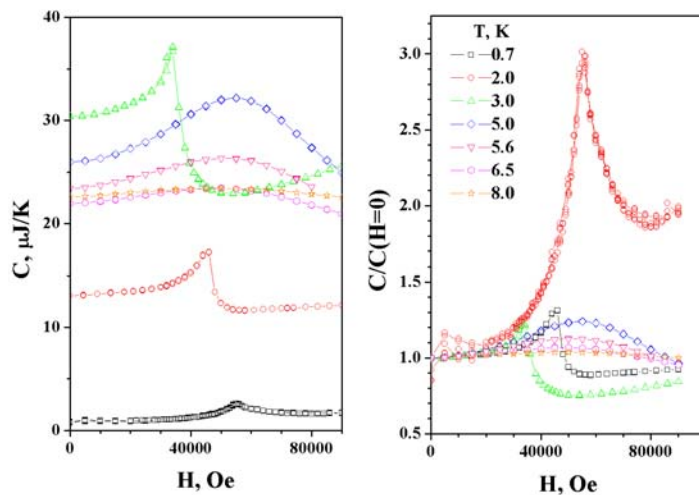


Fig. 4. Temperature dependence of the heat capacity of single crystal sample ( $m=1.78$  mg) of the triangular lattice antiferromagnet  $\text{RbFe}(\text{MoO}_4)_2$  at different in-plane magnetic fields.

In a previous study [3] we have investigated the main magnetic characteristics of  $\text{RbFe}(\text{MoO}_4)_2$ . During the course of the present project we performed a detailed calorimetric investigation of the  $H$ - $T$  phase diagram of this compound.

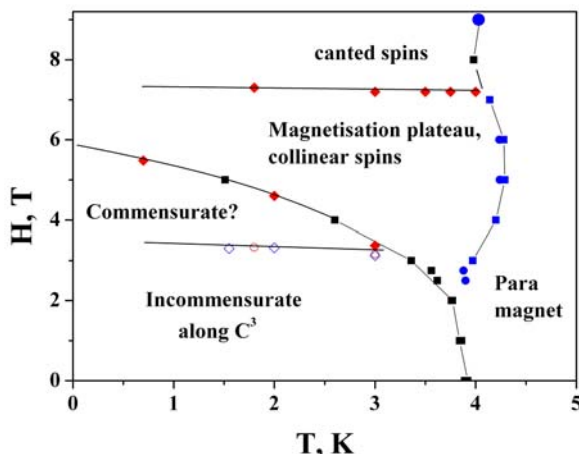
### Results

We have performed detailed heat capacity measurements in a magnetic field for several samples of  $\text{RbFe}(\text{MoO}_4)_2$ . Some of the results are shown in Figures 4 and 5.



The data obtained in heat capacity and magnetisation experiments allow us to refine the complicated phase diagram of  $\text{RbFe}(\text{MoO}_4)_2$  (Fig. 6), which appeared to possess features of a two dimensional triangular antiferromagnet (magnetisation plateau range, increase in the Néel temperature in a magnetic field) as well as additional phase transitions which we ascribe to three dimensional effects.

Fig.5. Field dependence of the specific heat of a single crystal of  $\text{RbFe}(\text{MoO}_4)_2$  ( $m=1.78$  mg). Magnetic field is aligned within a spin-plane.



### Resume

An experimental investigation of the phase transitions in a quasi-2D triangular lattice antiferromagnet revealed new previously unnoticed features of these phase transformations. A refined magnetic phase diagram has been obtained.

Fig. 6. Refined  $H$  vs  $T$  phase diagram of the quasi 2D triangular lattice antiferromagnet  $\text{RbFe}(\text{MoO}_4)_2$

### 2.3. Investigation of the magnetic phase transitions in the distorted triangular lattice antiferromagnet $\text{KFe}(\text{MoO}_4)_2$ .

#### Introduction

Compared to the case of  $\text{RbFe}(\text{MoO}_4)_2$  described above, a different situation is observed in  $\text{KFe}(\text{MoO}_4)_2$  crystals, where magnetic ordering takes place on a *distorted* triangular lattice. At a temperature of about 311 K, this compound exhibits a structural transition from a phase with a trigonal symmetry group to a monoclinic phase of  $C_{2h}^3$  symmetry. The size of the primitive cell along the Z-axis perpendicular to the magnetic layers doubles, and iron ions,  $\text{Fe}^{3+}_I$  and  $\text{Fe}^{3+}_{II}$ , appear in two nonequivalent positions. Owing to this decrease in the symmetry, we may expect that, at  $T < 311$  K, the exchange integral  $J_1$  for the neighbouring iron ions arranged along the X-axis will differ from the exchange integral  $J_2$  of the neighbours arranged along other directions in the triangular structure. Thus, the triangular structure of  $\text{KFe}(\text{MoO}_4)_2$  crystals is distorted and the crystals contain layers of magnetic ions occurring in the nonequivalent positions of two types. According to the theoretical analysis, a distortion corresponding to  $J_1 > J_2 > 0$  leads to the appearance of an incommensurate spiral structure with the wavevector oriented in the direction (X-axis) of distinct exchange interaction. In contrast, for  $J_1 > J_2/2 > 0$ , a collinear antiferromagnetic structure becomes energetically favourable. In this study we aimed to elucidate the effect of lattice distortions on the properties of 2D antiferromagnets on a triangular lattice.

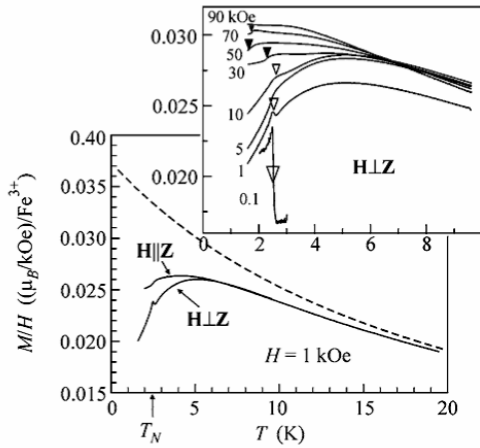


Fig. 7. The temperature dependence of the magnetic susceptibility of  $\text{KFe}(\text{MoO}_4)_2$  crystals.

#### Results

Figure 7 shows the temperature dependence of the magnetic susceptibility,  $\chi$ , of  $\text{KFe}(\text{MoO}_4)_2$  crystals for two orientations of the magnetic field:  $H \perp Z$  and  $H \parallel Z$ . At a temperature of  $T_N = 2.5$  K, the curves exhibit a feature corresponding to a transition to an ordered state. In the temperature interval  $15 \text{ K} < T < 300 \text{ K}$ ,  $\chi$  follows the Curie-Weiss law with the characteristic constant  $\Theta_{\text{CW}} = (21 \pm 2)$  K. The inset in Fig. 7 shows the temperature dependences of  $\chi$  for various values of the static field  $H$  oriented in the crystal plane. A peak is observed in the region of weak fields ( $0 < H < 20$  kOe) that is smeared in higher fields. Above 30 kOe, the  $M(T)$  curves exhibit variations in the form of steps, which are indicated by black triangles in the inset in Fig. 7.

Fig. 8 shows the  $M(H)$  curves measured at  $T = 1.6$  K for two orientations of the applied magnetic field. For  $H \perp Z$ , there are three features in these curves. Near  $H_{C1} = 12.5$  kOe, there is a change in the slope of the  $M(H)$  curve and the corresponding peak in the derivative  $dM/dH$ . The two other features are observed at  $H_{C2} = 52$  kOe and  $H_{C3} = 76$  kOe, where the derivative  $dM/dH$  exhibits sharp peaks. For  $H \parallel Z$ , the only special feature is an increase in the derivative in a field of 20–30 kOe. Fig. 9 presents the  $H$ - $T$  phase diagram showing the temperature variations of the fields of the magnetic phase transitions at  $H_{C1}$ ,  $H_{C2}$  and  $H_{C3}$ . It should be noted that the absence of a high-order axis also implies the presence of another, so-called “medium” magnetisation axis perpendicular to the hard axis. The results of these experiments show that the number of features of

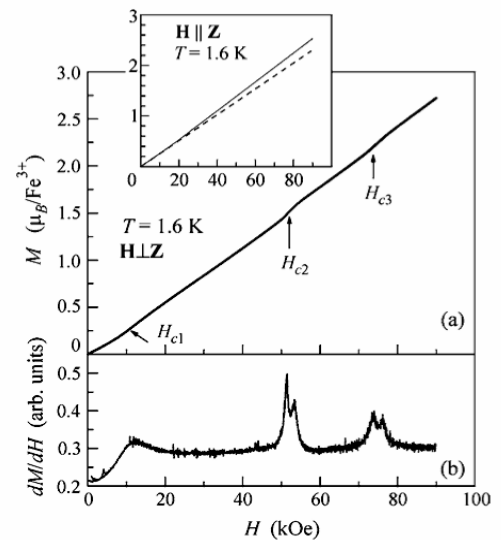


Fig. 8. The magnetization curve  $M(H)$  and its derivative measured for a  $\text{KFe}(\text{MoO}_4)_2$  crystal,  $H \perp Z$ ,  $T = 1.6$  K. The inset shows the  $M(H)$  curve observed for  $H \parallel Z$ .

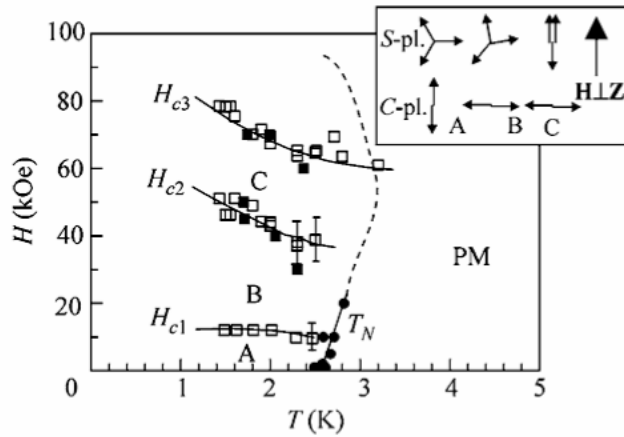


Fig. 9. The  $H$  versus  $T$  diagrams of the magnetic states observed for  $H \perp Z$ . The inset shows the probable spin structures of the magnetic phases A, B, and C.

to a rotation of the spin structure in the plane perpendicular to the hard axis. At the same time, the presence of phase transitions at the fields  $H_{C2}$  and  $H_{C3}$  are characteristic of the  $120^\circ$  triangular structure and the spiral structure on a distorted triangular lattice. The inset in Fig. 9 shows the scheme of probable spin configurations for the field orientation  $H \perp Z$ . The proposed model of a magnetic structure comprising of magnetic planes of two types (with collinear and spiral order) is also consistent with the results of our ESR measurements.

## Resume

The magnetic properties of a quasi-2D antiferromagnet on a distorted triangular lattice of  $\text{KFe}(\text{MoO}_4)_2$  have been studied. Magnetisation curves exhibit features corresponding to the spin-flop transition in a collinear biaxial antiferromagnet and simultaneously show a magnetisation plateau characteristic of a triangular spin structure. The experimental data are described in terms of a model comprising of alternating weakly bound magnetic layers, in which the main two exchange integrals have different values. Below the Neel temperature of 2.5 K, some of these layers possess a collinear antiferromagnetic structure, while the other layers have a triangular or spiral structure.

## 2.4. Adiabatic demagnetisation of a pyrochlore antiferromagnet $\text{Gd}_2\text{Ti}_2\text{O}_7$ .

### Introduction

Antiferromagnets on typical geometrically frustrated structures, such as kagome, garnet, and pyrochlore lattices, have an infinite number of classical ground states. This macroscopic degeneracy precludes any type of conventional magnetic ordering. As a result, frustrated magnets remain in a disordered cooperative paramagnetic ground state at temperatures well below the Curie-Weiss constant  $\Theta_{\text{CW}}$ . A number of geometrically frustrated magnets have been experimentally studied in the past decade.  $\text{Gd}_2\text{Ti}_2\text{O}_7$  (GTO) is one of the prototype examples, which yields a good realisation of a nearest-neighbour Heisenberg exchange antiferromagnet on a pyrochlore lattice. GTO remains disordered over a wide temperature interval below its  $\Theta_{\text{CW}}=10$  K. Infinite degeneracy of the magnetic ground state of a frustrated magnet implies the presence of a macroscopic number of local zero-energy modes. Such soft modes correspond to rotational degrees of freedom of a finite number

comparable magnitude in the  $M(H)$  curve exceeds the number expected for both collinear and spiral structures on a distorted triangular lattice. Indeed, only one (spin-flop) feature is expected for the collinear structure, and two such features (at the beginning and end of the magnetisation plateau) are expected for the triangular and spiral structures. The magnetic structure of  $\text{KFe}(\text{MoO}_4)_2$  comprises of two types of weakly bound alternating nonequivalent planes of magnetic ions. For this reason, we introduce a theoretical model in which collinear and spiral spin structures are formed in alternating planes.

Within the framework of this model, the low-field feature at  $H_{C1}$  can be viewed as a reorientational transition, which is related

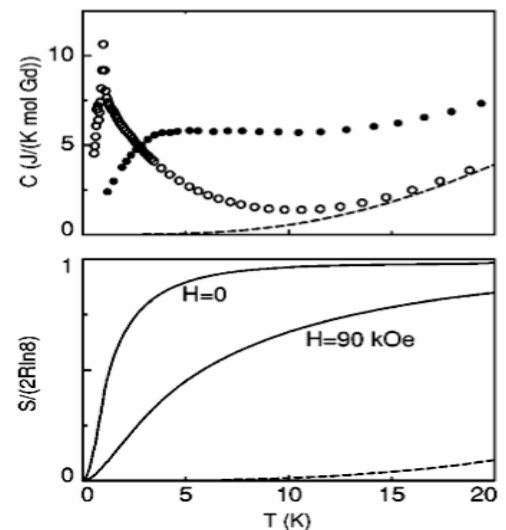


Fig. 10. Temperature dependence of the specific heat and the entropy of the  $\text{Gd}_2\text{Ti}_2\text{O}_7$  crystal. Solid lines are the results of  $C/T$  integration. Dashed lines represent the phonon contribution.

of a finite number

of spins with no change in the total exchange energy. An interesting effect related to a field evolution of the zero-energy local modes is an enhanced magnetocaloric effect near the saturation field  $H_{\text{SAT}}$  predicted in Ref. 5. Transformation between a nondegenerate fully polarised spin state above  $H_{\text{SAT}}$  and an infinitely degenerate magnetic state below  $H_{\text{SAT}}$  occurs via condensation of a macroscopic number of local modes and produces large changes of entropy in magnetic field.

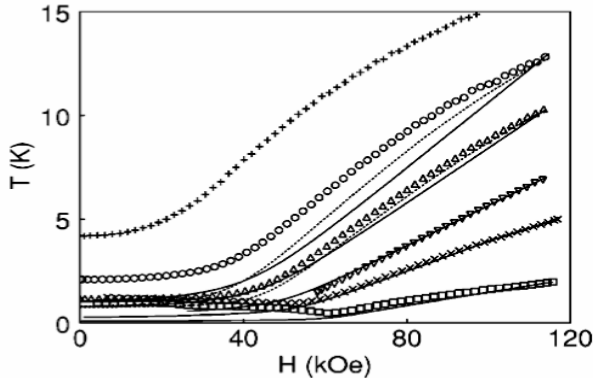


Fig. 11. Temperature variations of the adiabatic demagnetisation of  $\text{Gd}_2\text{Ti}_2\text{O}_7$  for various starting temperatures. Dotted lines show the corrections for the lattice heat capacity. Solid lines are obtained by Monte Carlo simulations.

## Experimental Details and Results

Specific heat measurements on a single-crystal sample of GTO performed in a zero field and at  $H=90$  kOe are presented in Fig. 10. Instead of the two sharp peaks seen in the zero field  $C(T)$  dependence at  $T_{\text{N1}}=1$  K and  $T_{\text{N2}}=0.75$  K corresponding to the ordering phase transitions, the high field curve contains a broad maximum around 5 to 6 K. The temperature dependence of the magnetic entropy obtained by integrating the  $C/T$  vs  $T$  curves is presented in the lower panel of Fig. 10. They give a general overview of the magnetocaloric effect in GTO. An adiabatic demagnetisation of the system down to zero field starting at  $H=90$  kOe and  $T=10$  K around  $\Theta_{\text{CW}}$  results in decrease in temperature down to 2 K, while the isothermal process at  $T=2$  K is

accompanied by an entropy increase of approximately one-half of the total magnetic entropy.

We have also performed direct measurements of the magnetocaloric effect in GTO by measuring the temperature of the sample in a quasiadiabatic regime as a function of time and magnetic field. A single-crystal GTO sample with a thermometer glued to it was suspended on four thin constantan wires in a vacuum chamber immersed in a helium bath. The heat exchange gas inside the chamber was absorbed by a charcoal. The temperature vs magnetic field curves for different starting temperatures are shown in Fig. 11.

The temperature drop on demagnetisation  $T_f/T_i$  depends on the starting temperature  $T_i$ . It has a maximum around  $T_i=10$  K, where the temperature drops by a factor of 10. A characteristic feature for all the curves starting below 10 K is that a great deal of cooling occurs in the field range from 120 to 60 kOe, which contrasts sharply with a continuous adiabatic cooling ( $T/H=\text{const}$ ) of an ideal paramagnet. Our results demonstrate the decisive role of the frustration in producing large adiabatic temperature changes in the pyrochlore. In typical nonfrustrated antiferromagnets, the magnetocaloric effect in the vicinity of field-induced transitions is very small.

The minimum temperature reached experimentally on demagnetisation from  $T_i=2$  K at  $H_f=62$  kOe is  $T_{\text{min}}=0.48$  K. This cooling limit is associated with the magnetic entropy freezing at the transition into an ordered state. When the field is further decreased, a weak temperature increase is observed.

## Resume

An adiabatic demagnetisation process is studied in  $\text{Gd}_2\text{Ti}_2\text{O}_7$ , a geometrically frustrated antiferromagnet on a pyrochlore lattice. In contrast to conventional paramagnetic salts, this compound can exhibit a temperature decrease by a factor of 10 in the temperature range below the Curie-Weiss constant. The most efficient cooling is observed in the field interval between 120 and 60 kOe corresponding to a crossover between the saturated and the spin-liquid phases. This phenomenon indicates that a considerable part of the magnetic entropy survives in the strongly correlated state.

## References

1. V.N. Glazkov, A.I. Smirnov, H.-A. Krug von Nidda, A. Loidl, K. Uchinokura, M. Masuda, Phys. Rev. Lett. **94**, 057205 (2005).
2. S. E. Korshunov, J. Phys. C **19**, 5927 (1986); D.H. Lee *et al.*, Phys. Rev. B. **33**, 450 (1986).
3. L. E. Svistov, A. I. Smirnov, L. A. Prozorova, O. A. Petrenko, L. N. Demianets and A. Ya. Shapiro, Phys. Rev. B **67**, 094434 (2003).
4. Masuda *et al.*, Phys. Rev. B **66**, 174416 (2002).
5. M.E. Zhitomirsky, Phys. Rev. B **67**, 104421 (2003).